HOKKAIDO UNIVERSITY

Title	Applicability of Butler Model for Estimation of Surface Tension in Liquid Na-K-Cs Alloys
Author(s)	Kawaguchi, Munemichi
Citation	Nuclear Technology https://doi.org/10.1080/00295450.2025.2502272
Issue Date	2025
Doc URL	https://hdl.handle.net/2115/97902
Rights	This is an Accepted Manuscript of an article published by Taylor & Francis in Nuclear Technology on 11 Jun 2025, available online: http://www.tandfonline.com/10.1080/00295450.2025.2502272.
Type	journal article
File Information	Manuscript.pdf

Hokkaido University Collection of Scholarly and Academic Papers : HUSCAP

Applicability of Butler Model for Estimation of Surface Tension in Liquid Na-K-Cs Alloys

Munemichi Kawaguchi[a]*

[a] *Division of Applied Quantum Science and Engineering, Hokkaido University, Sapporo, Japan;*

* Corresponding author

Name: Munemichi KAWAGUCHI

Affiliation: Division of applied quantum science and engineering, Hokkaido University

E-mail: kawaguchi.munemichi@eng.hokudai.ac.jp

Address: Kita 13, Nishi 8, Kita-ku, Sapporo, Hokkaido, 060-8628, Japan.

https://orcid.org/0000-0002-4038-565X

Applicability of Butler Model for Estimation of Surface Tension in Liquid Na-K-Cs Alloys

Thermodynamic calculation and evaluation of surface tension (σ) in ternary Na-K-Cs liquid were performed to investigate the Butler model's applicability with various geometric factors (L). The Butler model is a classic model used to evaluate the surface tension of binary and ternary liquids using thermodynamic data. In this study, the thermodynamic model incorporated binary Cs-K, Cs-Na, and Na-K models and a simple interaction energy model between ternary Na, K, and Cs. The phase diagrams and the activities obtained by the thermodynamic calculation were validated with the past experimental data. Furthermore, the surface tension evaluated using the Butler model with $L = 0.5L_0$ ($L_0 = 1.0$) was comparable to the experimental data with $\sigma + 0.02$ N/m and $\sigma - 0.01$ N/m. Furthermore, we compared the K-concentration dependence of the surface tension of Na-K liquids up to 600 K with that of the density function theory results. The $L = 0.5L_0$ gave us the best-estimated surface tensions in Na-K-Cs liquid.

Keywords: surface tension; alkali metal; fast reactor; coolant; thermodynamics calculation; Butler model;

Introduction

The Generation IV International Forum (GIF) selected six nuclear reactor systems as Generation IV technologies [1]. The coolant is a special issue: it is related to the operation temperature ranges, neutron capture cross-section, and compatibility with structural material and fuel in Table 1. In the proposed nuclear reactor systems, there are two liquid metal fast reactors (LMFR) such as sodium-cooled fast reactors (SFR) and lead-cooled fast reactors (LFR). For more than 60 years, sodium coolant has been used for fast breeder reactors in the world, such as EBR-2, Phenix, PFR, and MONJU. Simultaneously, research and development (R&D) of NaK coolant was conducted in EBR-1, BR-5, and DFR [2–7]. They show a good performance as heat transfer medium except for high chemical reactivity with water. Alkali metals and their alloys have unique

properties, such as high thermal conductivities, low melting points, and small ionization potential. Recently, the physical properties of ternary Na-K-Cs coolant, such as a thermo-chemical property, surface tension, and density, were measured to aim a low-melting multicomponent liquid-metal system, i.e., the low melting point was 195 K in atomic fractions of 0.139 Na-0.435 K-0.426 Cs [8–12]. In the case of lead and/or lead-bismuth eutectic (LBE) coolants, they do not have a high chemical reactivity but a corrosion behavior of structural material could be a problem [13]. Also, the LBE has been used for an accelerator-driven system as both a spallation target source and a coolant [14–16]. The R&Ds such as fluid simulation techniques and heat transfer problems have been conducted toward an engineering application.

The surface tension is one of the basic physical properties for fluid dynamics simulation, especially for the free interfacial fluid problem. Also, cohesion and adhesion on the solid-liquid interface are based on the surface tension. In the LMFR, fluid dynamics characteristics related to surface tension sometimes lead a safety issue [17–19]. However, there is a limited number of available experimental data of the surface tension, comparing with the density and viscosity etc. Then, it is important to validate the empirical equations in the mixture of liquids for the use. According to [20], the surface tension of LBE was investigated using the Butler model and/or geometric models that are new temperature scaling relationships. Butler model has been used extensively to calculate the surface tension of binary and ternary alloy systems [21–23]. In this model, the surface is treated as an additional thermodynamic phase with the bulk. By applying the simplest form of the quasi-chemical theory to the surface monolayer and directly using experimental values of the bulk activities, one can calculate the surface tension of binary alloys [24]. Based on the Butler model, the surface tension of liquid alloys, which are assumed to be the regular solution model, can be calculated.

In this study, we improved the Na-K-Cs thermodynamic models and validated the Na-K-Cs thermodynamic calculation results. Furthermore, we calculated the surface tension of binary Cs-K, Cs-Na, and Na-K liquids and ternary Na-K-Cs liquids by using the Butler model. Furthermore, its accuracy was evaluated by comparing the experimental data.

< Table 1 >

Thermodynamic model in Na-K-Cs liquid

Table 2 shows the thermodynamic model in Na-K-Cs liquid. The Gibbs energy function for the element i in phase φ was referred to the SGTE database [25] for pure elements (G_{Cs}^0, G_{Na}^0, and G_K^0). The thermodynamics of the binary liquid phase in the Cs-K, Cs-Na, and Na-K systems were used from Xin's model [26].

$$G_{ij} = x_i \ G_i^0 + x_j \ G_j^0 + RT\left(x_i \ lnx_i \ + x_j \ lnx_j \ \right) + G_{ij}^E \quad (1)$$

where $x_{i,j}$ is the molar fractions, and G_i^0 a molar Gibbs energy of the pure element i, respectively. R is the gas constant, T is the absolute temperature, and G_{ij}^E is the excess molar Gibbs energy expressed by the Redlich–Kister Polynomial:

$$G_{ij}^E = x_i \ x_j \ \sum_{k=0} L_{ij}^k \left(x_i \ - x_j \ \right)^k \quad (2)$$

where L_{ij}^k is the interaction energy coefficient between the elements i and j and takes the following form:

$$L_{ij}^k = A + BT \quad (3)$$

where the constants A and B are referred to Xin's model [26].

The intermetallic compounds of $CsNa_2$ and KNa_2 in the Cs–Na and the Na-K binary systems are modelled by a two-lattice model, $M_{1/3}N_{2/3}$ ($M =$ Cs or K and $N =$ Na). The Gibbs energy of the intermetallic compound is expressed by

$$G_{M;N} = \frac{1}{3}G_M^0 + \frac{2}{3}G_N^0 + A + BT \quad (4).$$

The A and B were referred to Xin's model [26].

The interaction energy of ternary phases in the Na-K-Cs system was investigated in [9–11, 27–29]. This study used the constant value, $L_{Cs,K,Na}^0 = -5000$ J/mol, as a simple model to reproduce the melting point.

< Table 2 >

Butler equation

The Butler equation has been used extensively to calculate the surface tension of binary and ternary alloys [22, 23]. The surface is assumed to be a monolayer, where the Gibbs energy is proportional to that of bulk liquid: $G_i^{Ex,S} = \beta G_i^{Ex,B}$. The β is the ratio between the two coordination numbers, which is often used as 0.83 in the case of metals. The super subscription, "*S*" and "*B*", denote surface and bulk phases. Based on the Butler model, the surface tension of liquid alloys is described by

$$\sigma = \sigma_i \ + \frac{RT}{S_i} ln \frac{x_i^S}{x_i^B} + \frac{1}{S_i}\left[G_i^{EX,S}\left(T, x_j^S\right) - G_i^{EX,B}\left(T, x_j^B\right)\right], \quad i,j = \text{Na, K, and Cs} \quad (5)$$

where σ_i J/m^2 and $S_i \ = L{N_0}^{1/3}{V_M}^{2/3}$ m^2/mol are the surface tension and the molar surface area of the pure element i, respectively. The L is a geometric factor in this study, N_0 1/mol is Avogadro's number, and V_M m^3/mol is the molar volume of element i. Also, the surface tension of ternary Na-K-Cs alloys is calculated using the surface tensions and molar surface area of binary Cs-Na alloy and K in this study. This method was applicable

for evaluating the surface tensions of complex multicomponent alloys, such as Fe-S-O and slags. The calculation results showed good agreement with the experimental data [30].

$$\sigma = \sigma_i \ + \frac{RT}{S_i} ln \frac{x_i^S}{x_i^B} + \frac{1}{S_i} \left[G_i^{EX,S}\left(T, x_j^S\right) - G_i^{EX,B}\left(T, x_j^B\right) \right], \quad i,j = \text{Cs-Na and K} \qquad (6)$$

where the Cs-Na alloy surface tensions were calculated using Equation (5) prior to calculating the Na-K-Cs alloy surface tensions. The Cs-Na alloy molar volume was referred to as the experimental values [10]. Table 3 shows the σ_i and V_M in the pure Cs, K, Na, and Cs-Na alloy liquid [28, 31]. To determine the multicomponent surface tension (σ), we calculate the apparent surface concentrations of each component using Equations (5) and/or (6).

< Table 3 >

This study compares calculated and experimental surface tensions (σ) at various temperatures and concentrations. Table 4 shows a summary table regarding the calculated and experimental σ with the reference.

< Table 4 >

Results and discussion

Thermodynamic calculation

Figure 1 shows phase diagrams of binary alkali metals obtained by the thermodynamic calculation, such as (a) Cs-K, (b) Cs-Na, and (c) Na-K systems. Fig. 1 reproduces the phase-diagram characteristics such as liquidus lines, solidus lines, and stable stoichiometric chemical compounds. In addition, Fig. 2 shows the thermodynamic activity of alkali metal components in (a) Cs-K, (b) Cs-Na, and (c) Na-K system at $T = 400$ K. The solid and dashed lines denote the present calculation results and the ideal solution model as a reference. The filled and open circles, triangles, and squares denote

the experimental values referred to [29, 32–34]. The present calculation results reproduced the experimental values very well. In conclusion, Figs. 1 and 2 revealed the validation of the binary-system thermodynamic model.

< Figure 1 >

< Figure 2>

Figure 3 shows the melting point in the ternary Na-K-Cs system. The contour plots and their temperature (K) are attached in Fig. 3. The lowest melting point is approximately 196 K, which was calculated at $x_{Na} = 0.16$, $x_K = 0.41$, and $x_{Cs} = 0.43$. The highest melting point is approximately T_m =371 K of pure Na melting point at $x_{Na} = 1.0$, $x_K = 0.0$, and $x_{Cs} = 0.0$. The melting point is distributed smoothly with the Na, K, and Cs concentrations. Especially, the melting point of K compounds depends on the Na concentration strongly because that of the pure Na element (T_m =371 K) is higher than those of pure K and Cs elements (T_m =337 K and 302 K). Furthermore, Fig. 3 agrees with the phase diagram suggested in [28]. It was revealed that the simple ternary interaction energy of $L^0_{Cs,K,Na} = -5000$ J/mol could calculate the thermodynamic characteristics at a whole range of Na, K, and Cs concentrations. Fig. 4 shows the Na, K, and Cs activities of ternary Na-K-Cs liquid at 373 K. They were obtained by thermodynamic calculation including the Table 2 interaction energy. The contour plots and the specific numbers are drawn in Fig. 4. Fig. 4 reveals that the activities of Na, K, and Cs depend strongly on each concentration, respectively. According to past experiments [29], the $a_{Na} = 0.260$, $a_K = 0.473$, $a_{Cs} = 0.465$ at $x_{Na} = 0.139$, $x_K = 0.435$, and $x_{Cs} = 0.426$ at 400 K. The activities of Na, K, and Cs, obtained by thermodynamic calculation at 400 K using this model, were $a_{Na} = 0.266$ $(+2.3\%)$, $a_K = 0.450$ (-4.9%), and $a_{Cs} = 0.433$ (-6.9%) at $x_{Na} = 0.139$, $x_K = 0.435$, and $x_{Cs} = 0.426$. The figures in the bracket show the difference between the past

experimental results and their calculation. The comparison of the phase diagram and their activities revealed the accuracy of the thermodynamic model using the parameters of Table 2.

< Figure 3 >

< Figure 4 >

Surface tension of Na-K-Cs liquids

Figure 5 shows the surface tensions (σ), the errors compared with the values of the experiments ($\frac{\sigma_{cal}-\sigma_{exp}}{\sigma_{cal}}$), and the apparent surface concentrations (x_i^S: i =Cs, K, and Na) of the binary alkali metal liquids such as (a) Cs-K, (b) Cs-Na, and (c) Na-K systems. In this study, we set the G_{ij}^E and the geometric factor as the ideal solution or Equation (2) and $L = L_0$ or $0.5L_0$ ($L_0 = 1.0$), respectively. The discussion section will discuss the $0.5L_0$ calculation because $L = L_0$ is usually used. The black solid and dashed lines and red line in Fig. 5 show the calculation results using $L = L_0$ or $0.5L_0$ and ideal solution model, respectively. The filled circles of the σ in Fig. 5 are the experimental data [28]. In the Cs-K system, the solid line ($L = L_0$) shows a good agreement with the experimental results. The average errors are 3.35% ($L = L_0$) and 6.62% ($L = 0.5L_0$). On the other hand, the solid lines ($L = L_0$) stand out as difference from the experimental results in the Cs-Na and the Na-K systems. Their average errors are 7.72% ($L = L_0$) and 3.69% ($L = 0.5L_0$) in the Cs-Na system and 4.40% ($L = L_0$) and 0.58% ($L = 0.5L_0$) in the Na-K system. In this study, we adapt $L = 0.5L_0$ for the calculation of the Butler equation considering that Na and Na-K are the actual coolant used in the fast reactors. Furthermore, in the apparent surface concentration, the dashed lines ($L = 0.5L_0$) showed the x_i^S is higher than the bulk concentration. Their x_i^S are caused mainly by the G_i^B but slightly by

the G_{ij}^{Ex} in all (a) Cs-K, (b) Cs-Na, and (c) Na-K systems. Namely, the apparent surface concentration denotes the effects of the excessive Gibbs energy of the surface.

< Figure 5 >

Fig. 6 shows the calculation results of the surface tensions of ternary Na-K-Cs liquids with (a) ideal solution model, (b) Equation (2) and $L = L_0$, and (c) Equation (2) and $L = 0.5L_0$ at $T = 373$K, respectively. In this ternary Na-K-Cs system calculation, we used the following calculation procedure. To compare the experimental data [28], Na_xCs_{1-x}-K (x =0, 0.22, 0.39, 0.43, 0.79, 0.85, 0.94, and 0.98), we recalculated the activities of the pseudo-binary Na_xCs_{1-x}-K systems from Fig. 4. Fig. 7 shows the activities of Na_xCs_{1-x} ($a_{Na_xCs_{1-x}}$) and K (a_K). The $a_{Na_xCs_{1-x}}$ was expressed by

$$a_{Na_xCs_{1-x}} = exp\left(-\frac{\mu_{Na_xCs_{1-x}} - \mu^0_{Na_xCs_{1-x}}}{RT}\right) \quad (6).$$

Here, μ_i is a chemical potential of component i. The bold lines of Fig. 7 show the a_{Cs}, a_K and a_{Na}. The $a_{Na_xCs_{1-x}}$ changed smoothly from the a_{Cs} to a_{Na}. In addition, we used the cross of the Cs-Na system in Fig. 5 as the $\sigma_{Na_xCs_{1-x}}$ in the Equation (5). The σ of the Na-K system was the highest in Fig. 6. The σ decreased as the Cs concentration increased. Furthermore, the σ of Na-K-Cs liquid showed a small downward peak along the K concentration due to the interaction energy between the elements. Fig. 8 shows the apparent surface concentration of x_K^S in the Na-K-Cs liquid. The x_K^S was obtained by the calculation of Equation (6). Fig. 9 shows the accuracy of the calculated σ. The horizontal axis is the experimental results and the vertical axis is the calculation results. The solid line ($y = x$) denotes that the calculation results match perfectly the experiment. The dashed lines are $y = x + 0.02$ and $y = x - 0.01$ in (a) Ideal solution model and (c) $L = 0.5L_0$ and $y = x + 0.015$ and $y = x - 0.028$ (b) $L = L_0$, respectively. As a whole, Fig.

9 shows that the Butler model calculation overestimates the experimental σ. The calculation accuracy in the low σ (high-K-concentration liquids) is less than in the high σ (high-Na-concentration liquids). It was within $\sigma + 0.02$ N/m and $\sigma - 0.01$ N/m in $L = 0.5L_0$.

< Figure 6 >

< Figure 7 >

< Figure 8 >

< Figure 9 >

K-concentration dependence of Na-K surface tension

Figure 10 shows the K-concentration dependence of Na-K surface tension at 371 K, which depends on (a) $L = 0.2L_0$–$1.0L_0$ ($L_0 = 1.0$) and (b) $\beta = 1/2$, $2/3$, $3/4$, 0.83, and 1.0, respectively. The solid lines and the filled circles were the Butler model calculation results and the experimental data at 373 K referred to [28], respectively. The open circles in Fig. 10 were the density function theory (DFT) calculation results at 373 K referred to [4]. Note that the DFT calculation was supposed to be a hyperbolic tangent concentration profile near the surface. It derived the rapid drop of σ near $x_K = 0$. Furthermore, the DFT calculations underestimated the Na and K surface tensions than the recommended experimentally σ [31]. The differences are 6.9% in Na and 1.1% in K, respectively. Therefore, the DFT calculation showed a lower σ than the experimental values and/or our calculation results in all x_K regions. The Butler model calculation results depend on the L but not the β. The slope of the surface tension for the K concentration increased gradually as the L decreased from $L = L_0$ to $L = 0.2L_0$. The surface tensions (σ_i) of the pure Na (at $x_K = 0$) and K (at $x_K = 1$) were not changed. The experimental results match the results of the Butler model calculation with $0.5L_0$

well. It is considered possible to select L in the Butler model for the best estimation of the empirical equation of the experimental data. On the other hand, the DFT calculation results were unreasonable with any of the Butler model calculation results.

< Figure 10 >

Temperature dependence of Na-K surface tension

Figure 11 shows Na-K surface tension at 371 K, 400 K, 450 K, and 600 K. The red solid, black solid, and dashed lines show the calculation results of the Na-K surface tensions with ideal solution model, $L = L_0$, and $L = 0.5L_0$, respectively. The filled circles and triangles show the experimental results [2, 27]. The open circles show the calculation results of the DFT [4]. Fig.11 revealed that the Butler model three cases overestimated the surface tension of the DFT at all temperatures. However, the DFT calculation results are smaller than the filled circles and/or the filled triangles, experimentally recommended σ_{Na} and σ_K of pure Na and K liquids in Table 3. The present calculation values were comparable to the filled triangles. According to the NaK handbook [2], the past experiments reported the surface tensions of eutectic NaK at the melting point were approximately 0.108 N/m by Weatherford et al. and 0.110 N/m by Bradhurst and Buchanan. Their values were ~0.103 N/m at 200ºC and ~0.099 N/m at 250 ºC, respectively. The experimental results have good agreement with the DFT calculation results. However, they were considered to include a large error because their values are far below pure Na and K surface tensions. The K-concentration dependence of the DFT calculation shows the similarity of Butler model calculation results with $L = L_0$. When Na liquid includes a few percentages of K contents, the Na-K surface tension decreases rapidly. Furthermore, as the liquid temperature is higher and higher, especially at 600 K, the K-concentration dependence matches the Butler model calculation results with $L =$

L_0. In the case of $L = 0.5L_0$, the slope of the surface tension for the K concentration is relatively larger. If the DFT calculation results have shifted by the difference of pure Na and K surface tensions, it would show agreement with the Butler model calculation results with $L = L_0$.

Kaptay improved the interfacial thermodynamic model and derived the most general equations to model interfacial energies [35].

$$\sigma = \frac{S_i}{S_i^M}\sigma_i \ + \frac{RT}{S_i^M} ln \frac{x_i^S}{x_i^B} + \frac{1}{S_i^M}\left[G_i^{EX,S}\left(T, x_j^S\right) - G_i^{EX,B}\left(T, x_j^B\right)\right], \quad i,j = \text{Na and K} \qquad (7)$$

Here, the S_i^M m^2/mol is the partial molar surface area of i. According to Kaptay, the difference between S_i and S_i^M is usually small, and in the first approximation, it can even be neglected ($S_i \ / S_i^M \approx 1$ in the first term in the right hand of Equation (7)). However, the S_i^M is not the standard molar surface area (S_i m^2/mol) of Na and K. The S_i^M should include the effects of the excessive molar Gibbs because the activity exists in real liquid alloys, as seen in Figs. 7. Furthermore, Fig. 5 revealed that Na-K alloy is the most significant difference between the experimental σ and the Butler calculation results with $L = L_0$, leading to the introduction of $L = 0.5L_0$ in Butler calculation. Furthermore, figs. 7 showed that the Na and K activities are the largest. Therefore, excess molar Gibbs energy is expected to contribute to the Na-K system's molar surface area (S_i^M). As a result, the $L = 0.5L_0$ gave us the best-estimated surface tensions in Na-K liquid. The Butler calculation with $L = 0.5L_0$ was especially close to the experimental values in 371 K. In general, the L values should depend on the G_i^{EX} and S_M.

< Figure 11 >

Conclusion

In this study, we improved the Na-K-Cs thermodynamic models and validated the Na-K-Cs thermodynamic calculation results, such as the Cs-K, Cs-Na, and Na-K phase diagrams, the melting point distribution in the Na-K-Cs system, and the activities (a_{Na}, a_K, and a_{Cs}). The thermodynamic model was incorporated by binary Cs-K, Cs-Na, and Na-K models and a simple interaction energy between ternary Na, K, and Cs. Furthermore, the evaluating surface tension (σ) in ternary Na-K-Cs liquid was performed to investigate the Butler model's applicability with various geometric factors (L). Considering that Na and Na-K are the actual coolant used in the fast reactors, the surface tension and its accuracy in ternary Na-K-Cs liquid by using the Butler model in three cases were evaluated. The surface tension evaluated using the Butler model with $L = 0.5L_0$ was comparable to the experimental data with an accuracy of $\sigma + 0.02$ N/m and $\sigma - 0.01$ N/m. Furthermore, we confirmed the Butler model's applicability in the high temperature, especially at 600 K. The Kaptay equation expects that the excess molar Gibbs energy contribute to the Na-K system's molar surface area. In this study, the $L = 0.5L_0$ gave us the best-estimated surface tensions in Na-K-Cs liquid.

Declaration of interest statement

No potential conflict of interest was reported by the author.

Reference

[1] Giorgio Locatelli, Mauro Mancini, Nicola Todeschini, "Generation IV nuclear reactors: Current status and future prospects," *Energy Policy*, **61**, 1503–1520 (2013); https://doi.org/10.1016/j.enpol.2013.06.101

[2] O. J. Foust, "Sodium-NaK engineering handbook. Volume I. Sodium chemistry and physical properties," NSA-27-012488 (Jan. 1972).

[3] C. T. Ewing, J. A. Grand, R. R. Miller, "Viscosity of the sodium–potassium system," *J. Phys. Chem.*, **58**, 12, 1086–1088 (1954); https://doi.org/10.1021/ja01147a086

[4] Wei-Heng Shih, D. Stroud, "Theory of the surface tension of liquid metal alloys," *Phys. Rev. B*, **32**, 804 (1985); https://doi.org/10.1103/PhysRevB.32.804

[5] O'Donnell, William J., Papanikolaou, Peter G., Reed, Claude B., "The thermophysical and transport properties of eutectic NaK near room temperature," ANL/FPP/TM—237 (Feb. 1989).

[6] K. Yu. Shunyaev, V. L. Lisin, "Calculation of Thermodynamic Properties and of Liquidus Line Positions for Na-K Alloys," *Journal of Thermal Analysis and Calorimetry*, **60**, 851–856 (2000); https://doi.org/10.1023/A:1010103623614

[7] E. E. Shpil'rain, V. I. Shkermontov, S. N. Skovorod'ko, A. G. Mozgovoi, "Activity of the Components of Binary Alloys of Alkali Metals: Na–K System," *High Temperature*, **40**, 33–43 (2002); https://doi.org/10.1023/A:1014230114968

[8] T. M. Taova, B. S. Karamurzov, F. M. Mal'surgenova, Kh. B. Khokonov, "Values of adsorption and surface concentrations of the components in Na-K-Cs alloys," *Bulletin of the Russian Academy of Sciences Physics*, **75**, 5, 2011; https://doi.org/10.3103/S1062873811050479

[9] N. E. Dubinin, "Thermodynamics of alkali metals melts," *Journal of Optoelectronics and Advanced Materials*, **5**, 5 (2003).

[10] T. M. Taova, F. M. Mal'surgenova, B. B. Alchagirov, Kh. L. Khokonov, "The density and molar volumes of ternary alloys of cross sections of the sodium-potassium-cesium system technically important temperatures," *Thermophysical Properties of Materials*, **47**, 815–821 (2009); https://doi.org/10.1134/S0018151X09060066

[11] E. E. Shpil'rain, S. N. Skovorod'ko, A. G. Mozgovoi, "The Activity of the Components of a Na–K–Cs System at High Temperatures," *High temperature*, **41**, 619–626 (2003); https://doi.org/10.1023/A:1026188410543

[12] R. Berg, M. Moldover, S. Rabinovich, A. Voronel, “Viscosity and density of two alkali metal mixtures,” *Journal of Physics F-Metal Physics*, **17**, 9, 18761 (1987); DOI 10.1088/0305-4608/17/9/012

[13] Jinsuo Zhang, Ning Li, “Review of the studies on fundamental issues in LBE corrosion,” *Journal of Nuclear Materials*, **373**, 1–3, 351–377 (2008); https://doi.org/10.1016/j.jnucmat.2007.06.019

[14] Kenji Kikuchi, Shigeru Saito, Yuji Kurata, Masatoshi Futakawa, Toshinobu Sasa, Hiroyuki Oigawa, Eiichi Wakai, Makoto Umeno, Hiroshi Mizubayashi, Kuniaki Miura, “Lead-Bismuth Eutectic Compatibility with Materials in the Concept of Spallation Target for ADS,” *JSME International Journal Series B Fluids and Thermal Engineering*, **47**, 2, 332–339 (2004);

[15] Shinya Miyahara, Naoya Odaira, Yuji Arita, Fujio Maekawa, Hiroki Matsuda, Toshinobu Sasa, Shin-ichiro Meigo, “The analytical study of inventories and physicochemical configuration of spallation products produced in Lead-Bismuth Eutectic of Accelerator Driven System,” *Nucl. Eng. Design.*, **352**, 110192 (2019); https://doi.org/10.1016/j.nucengdes.2019.110192

[16] Koji Morita, Werner Maschek, Michael Flad, Hidemasa Yamano, Yoshiharu Tobita, “Thermophysical Properties of Lead-Bismuth Eutectic Alloy in Reactor Safety Analyses,” *J. Nucl. Sci. Technol.*, **43**, 5, 526–536 (2006); https://doi.org/10.1080/18811248.2006.9711131

[17] Munemichi Kawaguchi, Yasushi Hirakawa, Yusuke Sugita, Yutaka Yamaguchi, “Estimation Method for Residual Sodium Amount on Unloaded Dummy Fuel Assembly,” *Nucl. Technol.*, **210**, 1, 55–71 (2024); https://doi.org/10.1080/00295450.2023.2214261

[18] K. Satpathy, K. Velusamy, B.S.V. Patnaik, P. Chellapandi, “Numerical simulation of liquid fall induced gas entrainment and its mitigation,” *International Journal of Heat and Mass Transfer*, **60**, 392–405 (2013); https://doi.org/10.1016/j.ijheatmasstransfer.2013.01.006

[19] C. Peng, D.L. Qiao, D. Li, J. Wu, “Liquid spray modeling under sodium fire accidents,” *Nuclear Engineering and Design*, **379**, 11260 (2021); https://doi.org/10.1016/j.nucengdes.2021.111260

[20] Yu. Plevachuk V. Sklyarchuk, G. Gerbeth, S. Eckert, R. Novakovic, “Surface tension and density of liquid Bi–Pb, Bi–Sn and Bi–Pb–Sn eutectic alloys,” *Surface Science*, **605**, 1034–1042 (2011); https://doi.org/10.1016/j.susc.2011.02.026

[21] Butler, J. A. V., "The Thermodynamics of the Surfaces of Solutions," *Proceedings of the Royal Society of London. Series A, Containing Papers of a Mathematical and Physical Character*, **135**, 827, 348–375 (Mar. 1932);

[22] K. S. Yeum, R. Speiser, D. R. Poirier, "Estimation of the surface tensions of binary liquid alloys," *Metallurgical Transactions B*, **20**, 693–703, (1989); https://doi.org/10.1007/BF02655927

[23] Toshihiro Tanaka, Tomoko Kitamura, Ida Annika Back, "Evaluation of Surface Tension of Molten Ionic Mixtures," *ISIJ International*, **46**, 3, 400–406 (2006); https://doi.org/10.2355/isijinternational.46.400

[24] George Kaptay, "Improved Derivation of the Butler Equations for Surface Tension of Solutions," *Langmuir*, **35**, 33 (2019); https://doi.org/10.1021/acs.langmuir.9b01892

[25] A.T. Dinsdale, "SGTE data for pure elements," *Calphad*, **15**, 4, 317–425 (1991); https://doi.org/10.1016/0364-5916(91)90030-N

[26] Xin Ren, Changrong Li, Zhenmin Du, Cuiping Guo, "Thermodynamic assessments of six binary systems of alkali metals," *Calphad*, **35**, 3, 446–454 (2011); https://doi.org/10.1016/j.calphad.2011.06.005

[27] N.E. Dubinin, A.A. Yuryev, N.A. Vatolin, "Thermodynamic Properties of Ternary Liquid Metal Alloys," *High Temperature Materials and Processes*, **14**, 4, 285–290 (2011); https://doi.org/10.1515/HTMP.1995.14.4.285

[28] T. M. Taova, B. S. Karamurzov, B. B. Alchagirov, R. Kh. Arkhestov, Kh. B. Khokonov, "Liquid-metal coolants for fast neutron reactors: Liquidus surface tension," *Inorganic Materials: Applied Research*, **1**, 133–138 (2010); https://doi.org/10.1134/S2075113310020103

[29] D N Kagan, G A Krechetova, E E Shpilrain, "Elaborating and applying a new method of Gibbs energy determination for multicomponent alkali-metal coolants," *J. Phys.: Conf. Ser.*, **98**, 032007 (2008)

[30] Joonho Lee, Kazuki Morita, " Effect of carbon and sulfur on the surface tension of molten iron," *Process metallurgy*, **73**, 9, 367–372 (2002); https://doi.org/10.1002/srin.200200001

[31] Ohse, R W, *Handbook of thermodynamic and transport properties of alkali metals*, 6.3.3 Density and thermal expansion, p. 435–470, International Union of pure and applied chemistry, United Kingdom (1985).

[32] Fred A. Cafasso, Vishwa M. Khanna, H.M. Feder, “Thermodynamic properties and ordering in liquid NaK alloys,” *Advances in Physics*, **16**, 63, 535–543 (2006); https://doi.org/10.1080/00018736700101645

[33] K. Ichikawa, S. M. Granstaff, Jr., J. C. Thompson, “Chemical potentials and related thermodynamics of liquid Na–Cs alloys,” *The Journal of Chemical Physics*, **61**, 4059–4062 (1974); https://doi.org/10.1063/1.1681699

[34] F E Neale, N E Cusack, “Thermodynamic properties of liquid sodium-caesium alloys,” *Journal of Physics F: Metal Physics*, **12**, 2839–2850 (1982); https://doi.org/10.1088/0305-4608/12/12/016

[35] George Kaptay, “A coherent set of model equations for various surface and interface energies in systems with liquid and solid metals and alloys,” *Advances in Colloid and Interface Science*, **283**, 102212 (2020); https://doi.org/10.1016/j.cis.2020.102212

Table 1. Characteristics of coolant in Generation IV nuclear reactors [1].

Reactor	Coolant	Characteristics
Sodium fast reactor (the most researched type of fast reactor)	Sodium	- A lower melting point (98 ºC) and less corrosive than the lead alternative - High specific heat - Low pressurisation of the RPV - React with air and water
Lead cooled fast reactor	Lead or lead-bismuth eutectic (LBE)	- A low melting point (327 ºC for lead and 125 ºC for LBE) - A high boiling point (1743 ºC for lead and 1670 ºC for LBE) - Excellent neutron and thermo-fluid-dynamic properties (natural convection in the RPV) - Corrosive the structural materials - Not react with air and water
Super-critical water cooled reactor	Supercritical water	- Requirement of R&Ds of the chemistry of irradiated supercritical water and its thermal fluid dynamic behavior - High pressurisation of the RPV
Very high temperature reactor Gas cooled fast reactor	Helium	- A low specific heat - Radiologically and chemically inert gas - Stable in all relevant thermodynamic conditions
Molten salt reactor	Molten salts	- High melting point (about 500 ºC) - Thermal stability at high temperatures (above 800 ºC) - High specific heat - Low pressurisation of the RPV - Requirement for removing lanthanides, noble gases, and noble melts - Corrosive the structural materials - Not react with air and water

RPV: Reactor pressure vessel

Table 2. Thermodynamic model in Na-K-Cs liquid.

Elements	Phase	Model	$L^{i}_{M,N}$, $G_{M;N}$ (J/mol)
Cs -K [26]	Liquid	(Cs, K)	$L^{0}_{Cs,K} = 426.310 - 0.289T$ $L^{1}_{Cs,K} = -173.221 + 1.348T$ $L^{2}_{Cs,K} = 177.307 - 1.339T$
	BCC (A2)	(Cs, K)	$L^{0}_{Cs,K} = 4120.709 - 6.131T$ $L^{1}_{Cs,K} = -365.975 - 0.036T$
Cs -Na [26]	Liquid	(Cs, Na)	$L^{0}_{Cs,Na} = 3603.202 + 0.299T$ $L^{1}_{Cs,Na} = -2274.182 + 0.150T$ $L^{2}_{Cs,Na} = 1463.096 - 1.509T$
	$CsNa_2$	$(Cs)_{1/3}(Na)_{2/3}$	$G_{Cs;Na} = 1/3\,G^{0}_{Cs} + 2/3\,G^{0}_{Na} - 478.531 + 1.222T$
Na-K [26]	Liquid	(K, Na)	$L^{0}_{K,Na} = 2938.543 + 0.413T$ $L^{1}_{K,Na} = -748.741 + 1.432T$ $L^{2}_{K,Na} = 240.989 - 1.304T$
	BCC (A2)	(K, Na)	$L^{0}_{K,Na} = 11799.512 - 10.004T$ $L^{1}_{K,Na} = -1298.161 - 1.000T$
	KNa_2	$(K)_{1/3}(Na)_{2/3}$	$G_{K;Na} = 1/3\,G^{0}_{K} + 2/3\,G^{0}_{Na} + 10.126 - 0.921T$
Na-K-Cs	Liquid	(Cs, K, Na)	$L^{0}_{Cs,K,Na} = -5000$

Table 3. Molar volume (V_{M}) [31] and surface tension ($\sigma_i(T)$) [28] of Na, K, and Cs elements with T (K).

Elements	Molar volume, V_{M} (m^3/mol)	Surface tension, $\sigma_i(T)$ (N/m^2)
Na	$\frac{M_{Na}}{\sum_{i=0}^{6} a_i\,(T/1000)^i}$	$0.205 - 0.094 \times 10^{-3}(T - 370.99)$
K	$\frac{M_K}{\sum_{i=0}^{6} b_i\,(T/1000)^i}$	$0.116 - 0.062 \times 10^{-3}(T - 336.45)$
Cs	$\frac{M_{Cs}}{\sum_{i=0}^{6} c_i\,(T/1000)^i}$	$0.075 - 0.050 \times 10^{-3}(T - 301.49)$
Cs-Na	$\sum_{i=0}^{4} d_i\,{x_{Na}}^i$	This study used the calculation results from Equation (5).

Coefficients of polynomial approximate equations for liquid Na, K, and Cs [31]: $a_0 = 1.01503$, $a_1 = -0.23393$, $a_2 = -0.00305$, $a_i = 0$ $(i = 3-6)$, $b_0 = 0.91474$, $b_1 = -0.27731$, $b_2 = 0.09814$, $b_3 = -0.10186$, $b_4 = 0.05179$, $b_5 = -0.01216$, $b_6 = 0$, $c_0 = 2.02678$, $c_1 = -0.61200$, $c_2 = -0.20233$, $c_3 = 0.84066$, $c_4 = -1.10010$, $c_5 = 0.60684$, $c_6 = -0.12500$, $d_0 = 0.07362$, $d_1 = -0.05705$, $d_2 = 0.00542$, $d_3 = 0.00032$, $d_4 = 0.00309$, $d_i = 0$ $(i = 5-6)$. Atomic mass: M_i (i =Na, K, and Cs)

Table 4. A summary table comparing calculated and experimental surface tensions (σ). The square bracket denotes the source where [Present] is this work and [*] is reference number.

Figure	Calculation	Experiment
5(a)	[Present] Cs-K σ of 373K using L_0 and $0.5L_0$.	[28] Cs-K σ of 373 K.
5(b)	[Present] Cs-Na σ of 373K using L_0 and $0.5L_0$.	[28] Cs-Na σ of 373 K.
5(c)	[Present] Na-K σ of 373K using L_0 and $0.5L_0$.	[28] Na-K σ of 373 K.
6	[Present] Na-K-Cs σ of 373K using $0.5L_0$.	[28] Na-K-Cs σ of 373 K.
9	[Present] Na-K-Cs σ of 373K using $0.5L_0$.	[28] Na-K-Cs σ of 373 K.
10	[Present] Na-K σ of 371K using $0.2L_0$–$1.0L_0$.	[23] Na-K σ of 373 K.
	[4] Na-K σ of 371K using DFT.	
	[Present] Na-K σ of 371K using L_0 and $0.5L_0$.	[23] Na-K σ of 373 K.
11(a)	[Present] Na-K σ of 371K using Kaptay eq.	
	[4] Na-K σ of 371K using DFT.	
	[Present] Na-K σ of 400K using L_0 and $0.5L_0$.	[31] Na and K σ of 400 K.
11(b)	[Present] Na-K σ of 400K using Kaptay eq.	
	[4] Na-K σ of 400K using DFT.	
	[Present] Na-K σ of 450K using L_0 and $0.5L_0$.	[31] Na and K σ of 450 K.
11(c)	[Present] Na-K σ of 450K using Kaptay eq.	[2] Na_2K σ of 473 K and 523 K.
	[4] Na-K σ of 450K using DFT.	
	[Present] Na-K σ of 600K using L_0 and $0.5L_0$.	[31] Na and K σ of 600 K.
11(d)	[Present] Na-K σ of 600K using Kaptay eq.	
	[4] Na-K σ of 600K using DFT.	

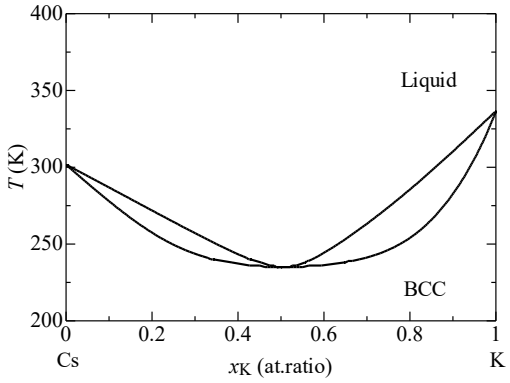

(a) Cs-K system

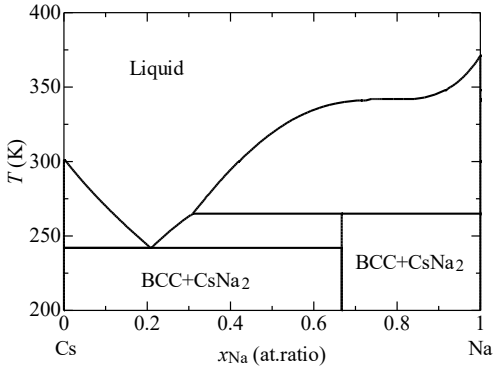

(b) Cs-Na system

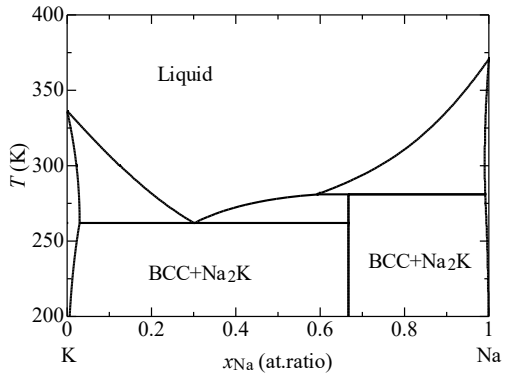

(c) Na-K system

Figure 1. Binary-alkali-metal phase diagrams [26] calculated in this work: (a) Cs-K, (b) Cs-Na, and (c) Na-K systems.

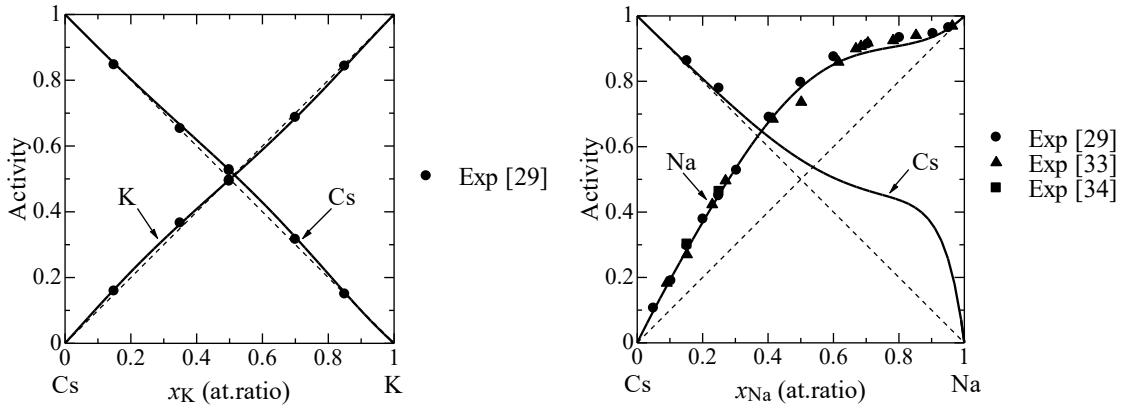

(a) Cs-K

(b) Cs-Na

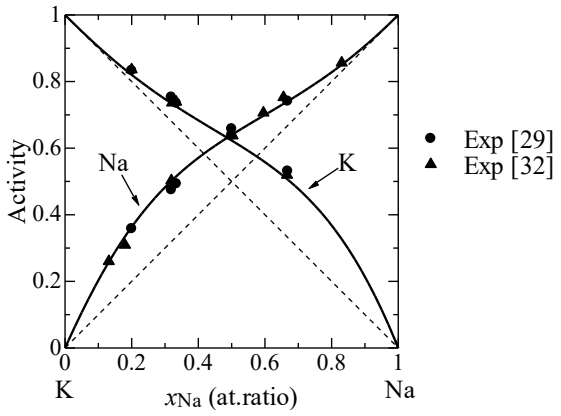

(c) Na-K

Figure 2. The thermodynamic activity of alkali metal component in binary systems at $T = 400$ K: (a) Cs-K, (b) Cs-Na, and (c) Na-K system.

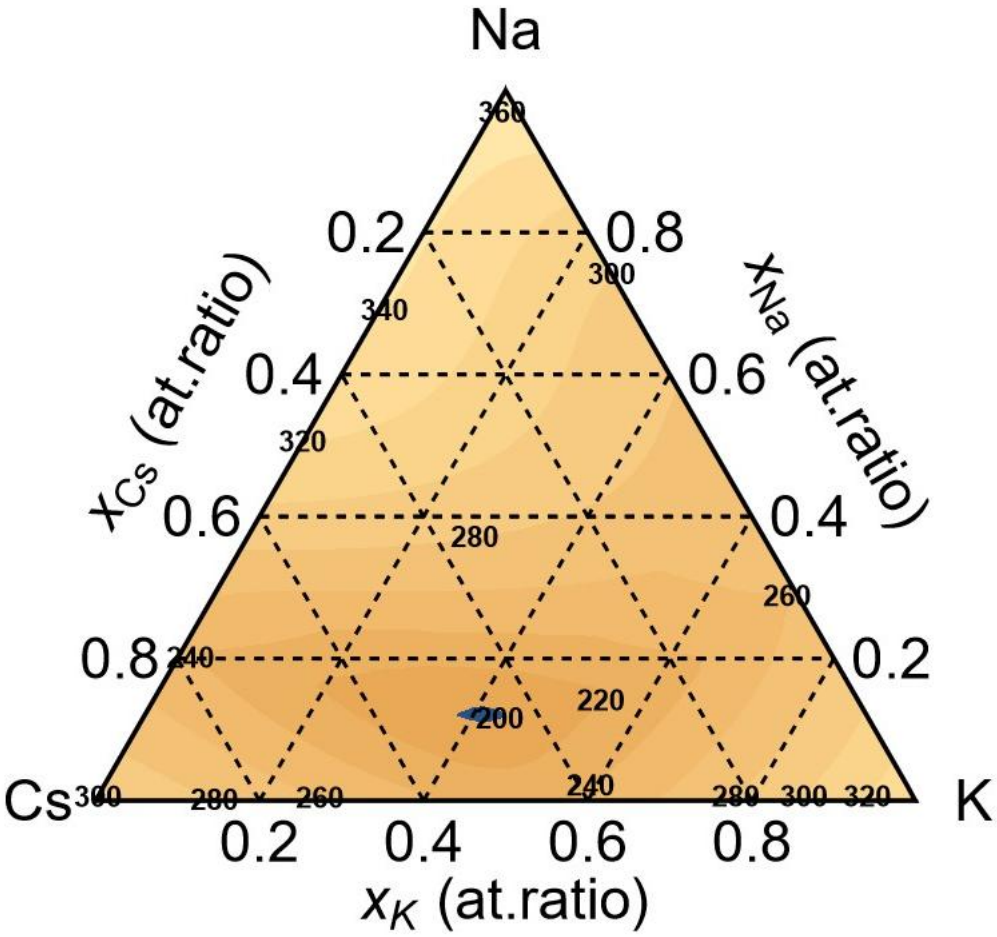

Figure 3. Melting point (T_m K) in ternary Na-K-Cs system.

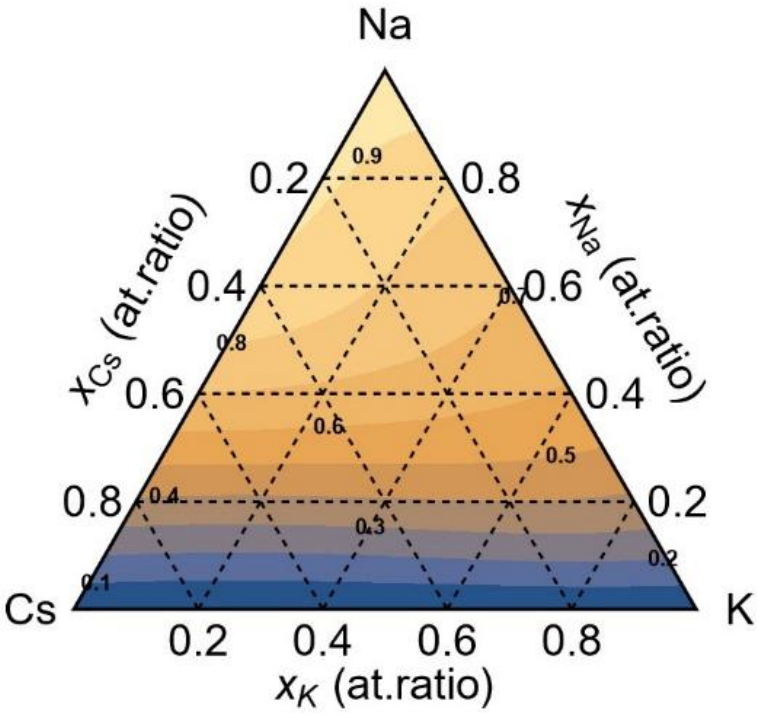

(a) Na activity

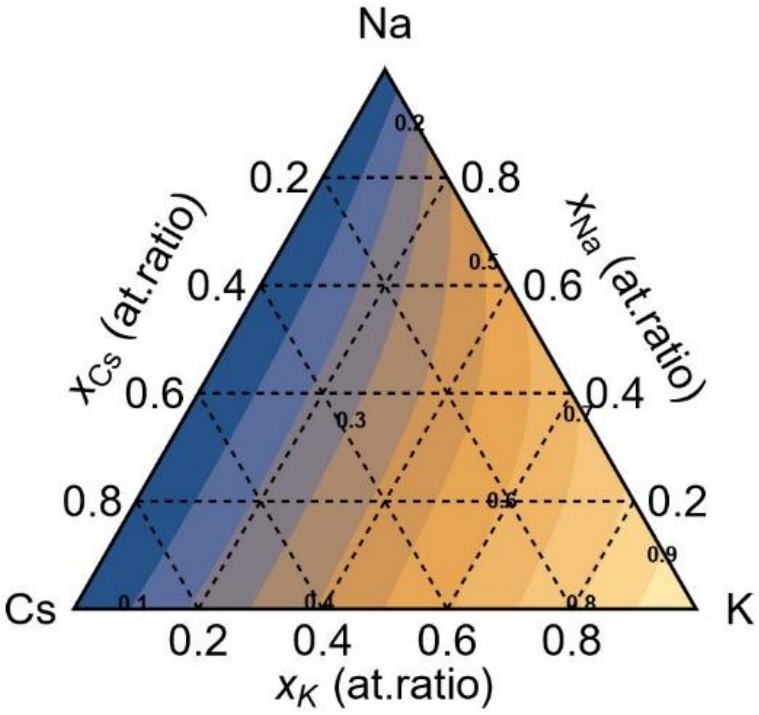

(b) K activity

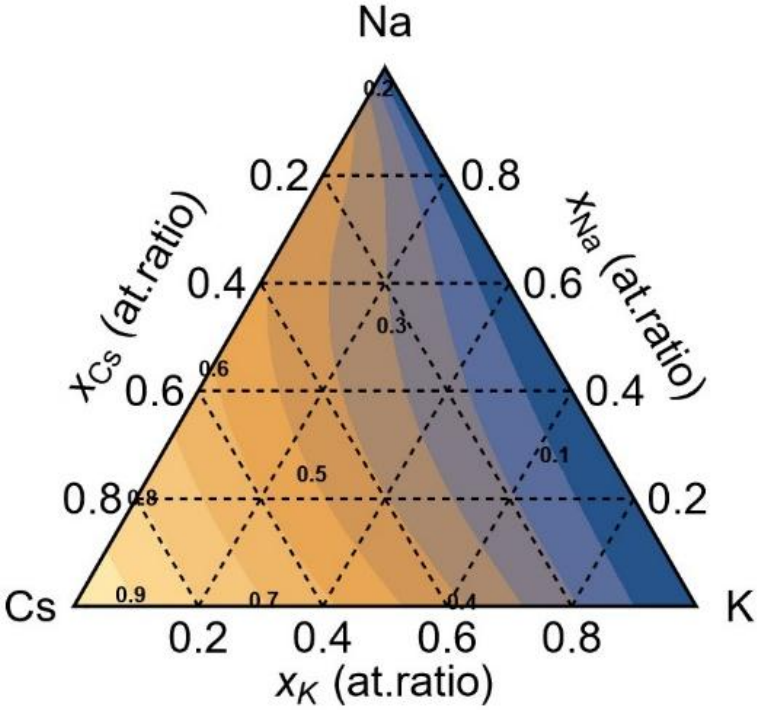

(c) Cs activity

Figure 4. Thermodynamic activities of alkali metal components in ternary Na-K-Cs system at $T = 373$ K: (a) Na, (b) K, and (c) Cs activities.

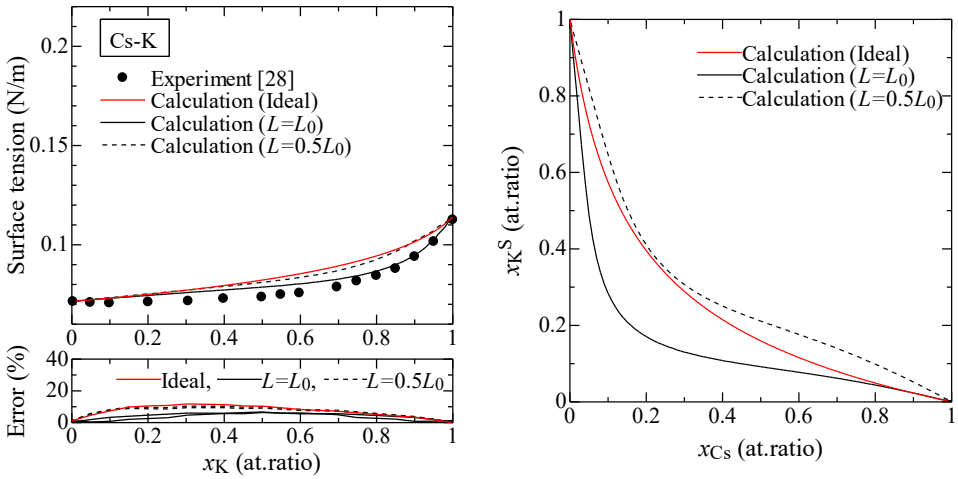

(a) Cs-K

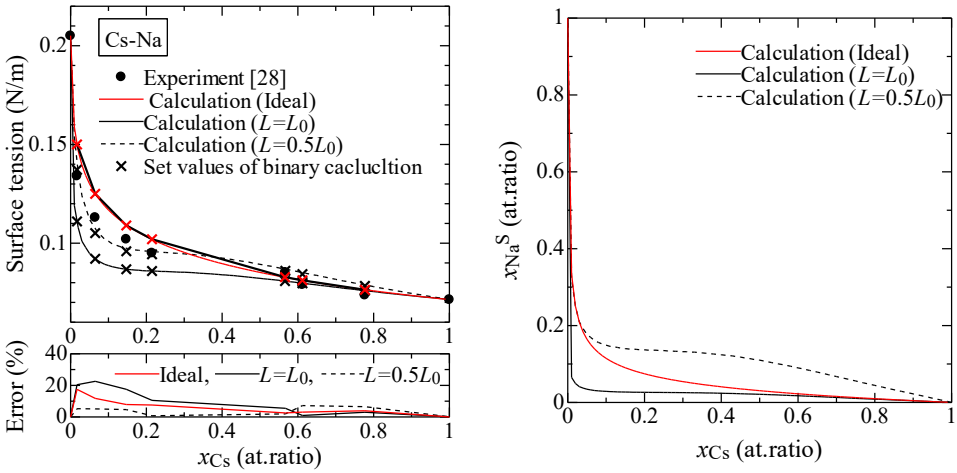

(b) Cs-Na

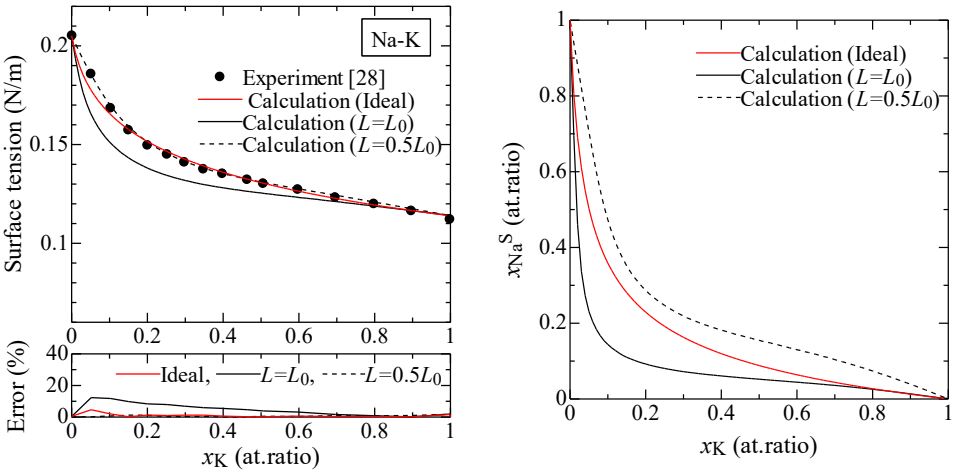

(c) Na-K

Figure 5. Surface tensions of Cs-K, Cs-Na, and Na-K liquids at $T = 373$ K, which were calculated under the condition of the binary Na_xCs_{1-x}-K systems. Error denotes the difference between the calculation and the experiment.

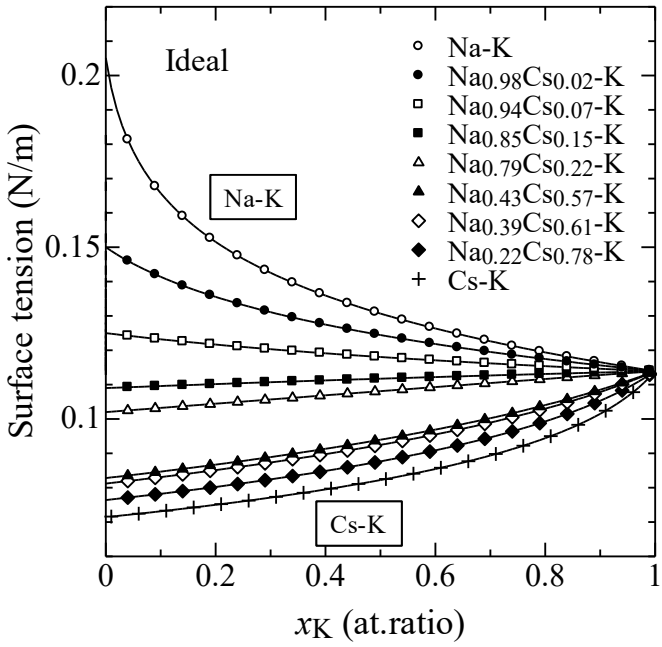

(a) Ideal solution

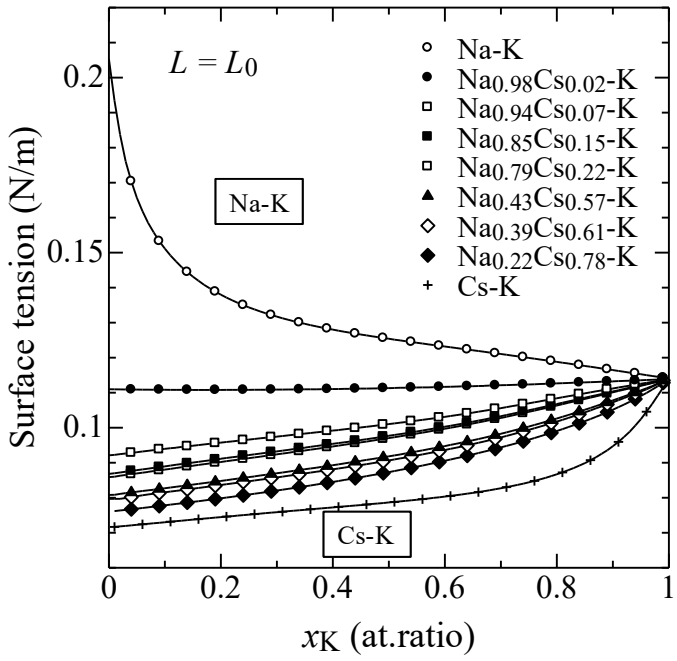

(b) $L = L_0$

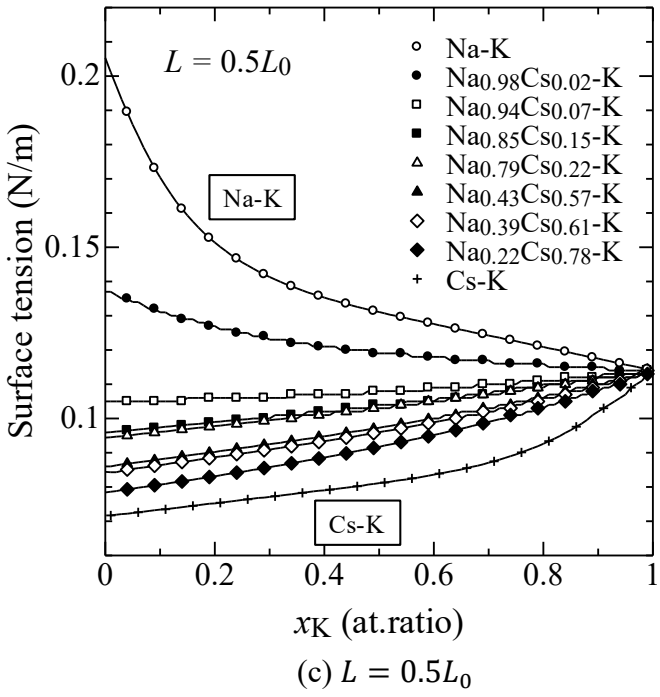

(c) $L = 0.5L_0$

Figure 6. Surface tensions of Na-K-Cs liquids at $T = 373$ K, which were calculated under the conditions of binary Na_xCs_{1-x}-K systems.

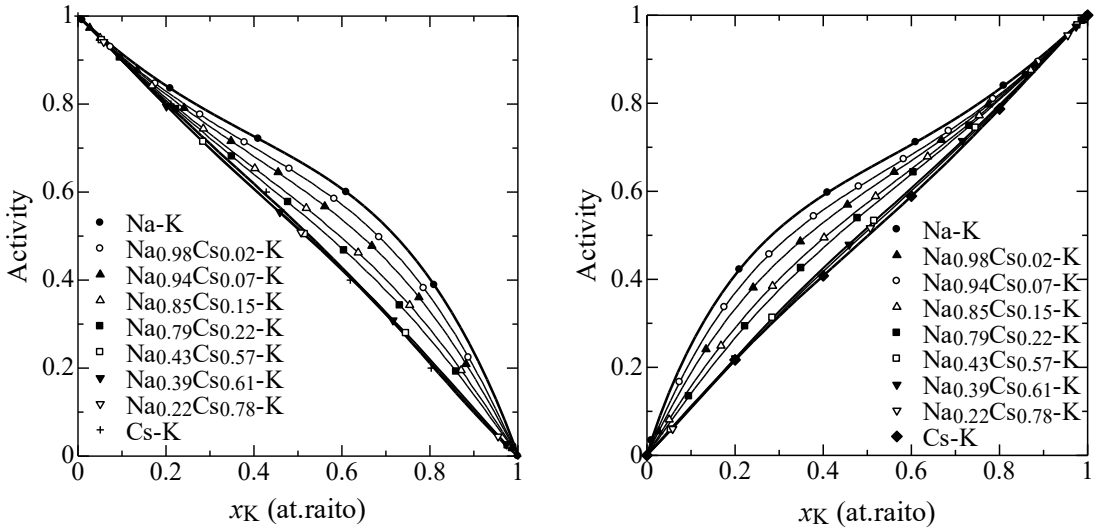

(a) Na_xCs_{1-x} activity ($a_{Na_xCs_{1-x}}$)

(b) K activity (a_K)

Figure 7. Thermodynamic activities of Na_xCs_{1-x} and K components in ternary Na-K-Cs system at $T = 373$ K.

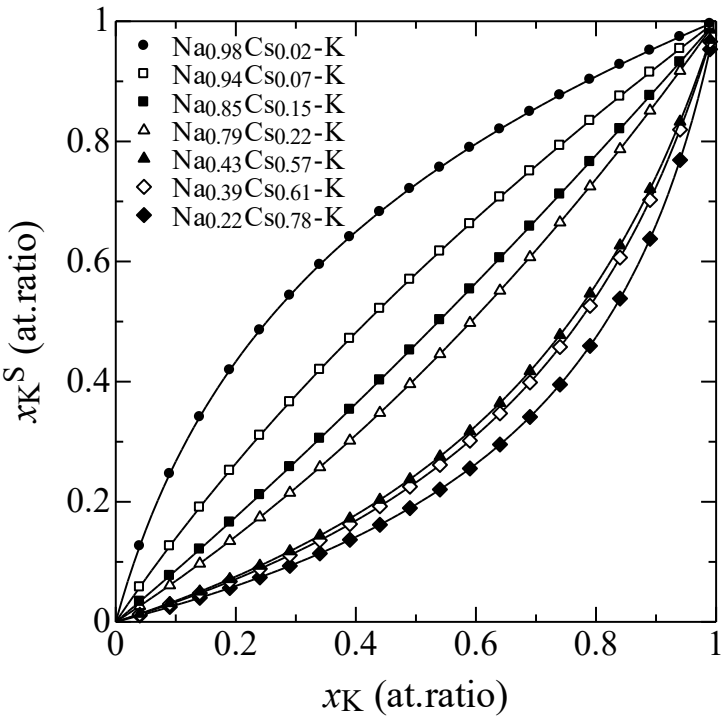

(a) Ideal solution

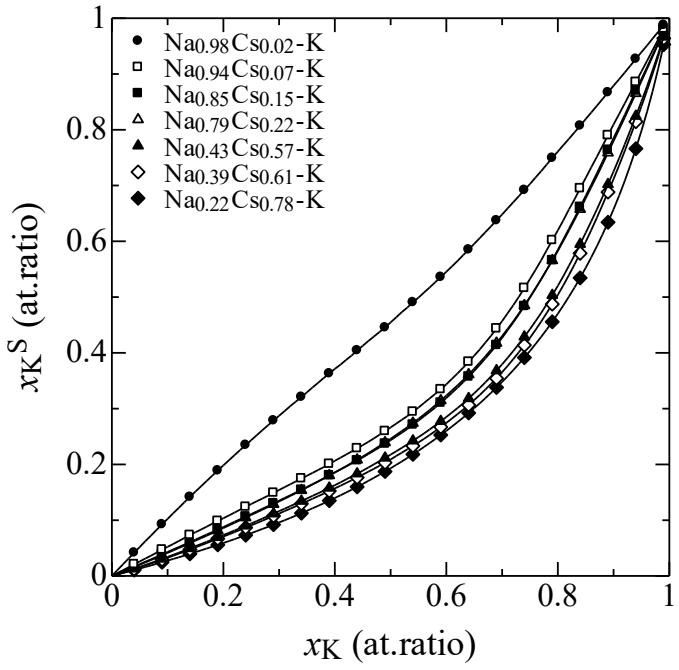

(b) $L = L_0$

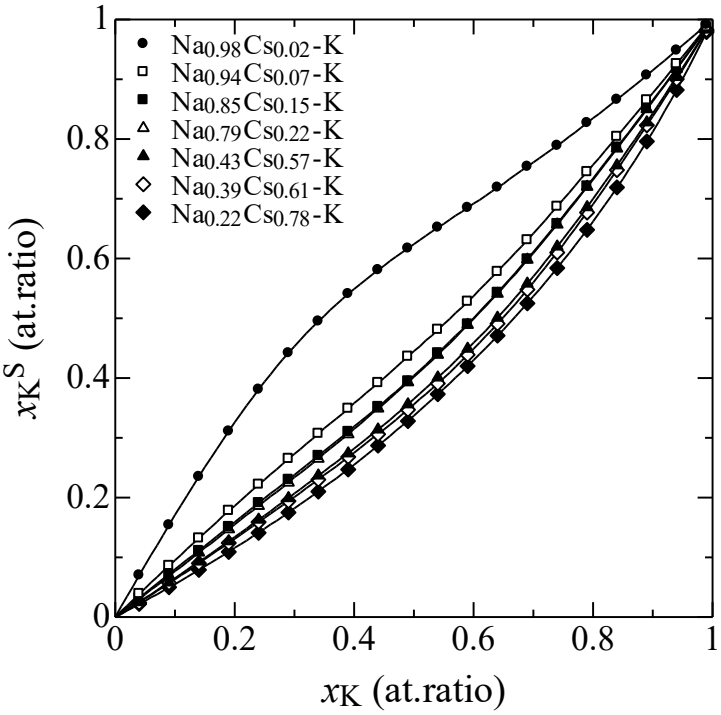

(c) $L = 0.5L_0$

Figure 8. The surface concentration of the K component (x_K^S) in Na_xCs_{1-x}-K ($x = 0.22$, 0.39, 0.43, 0.79, 0.85, 0.94, 0.98) at $T = 373$ K.

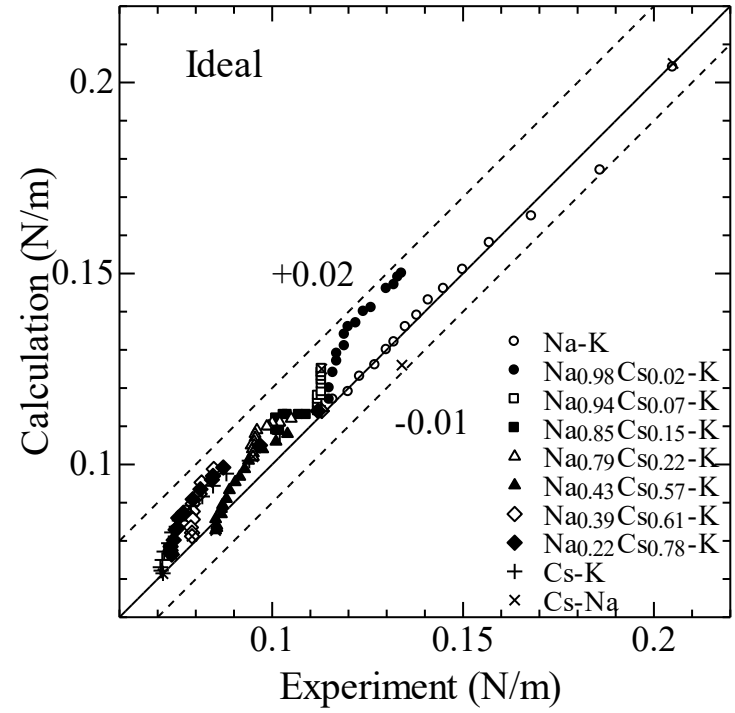

(a) Ideal solution

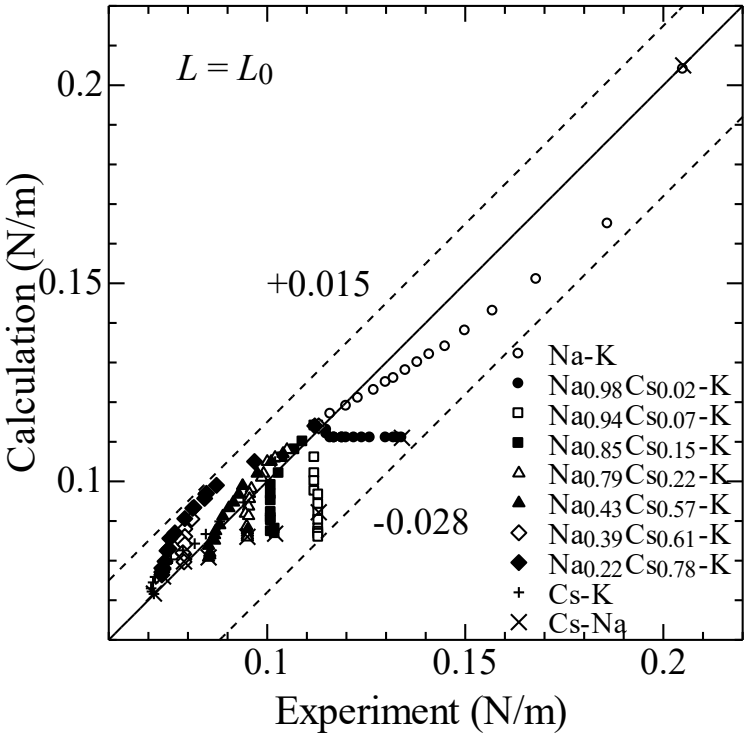

(b) $L = L_0$

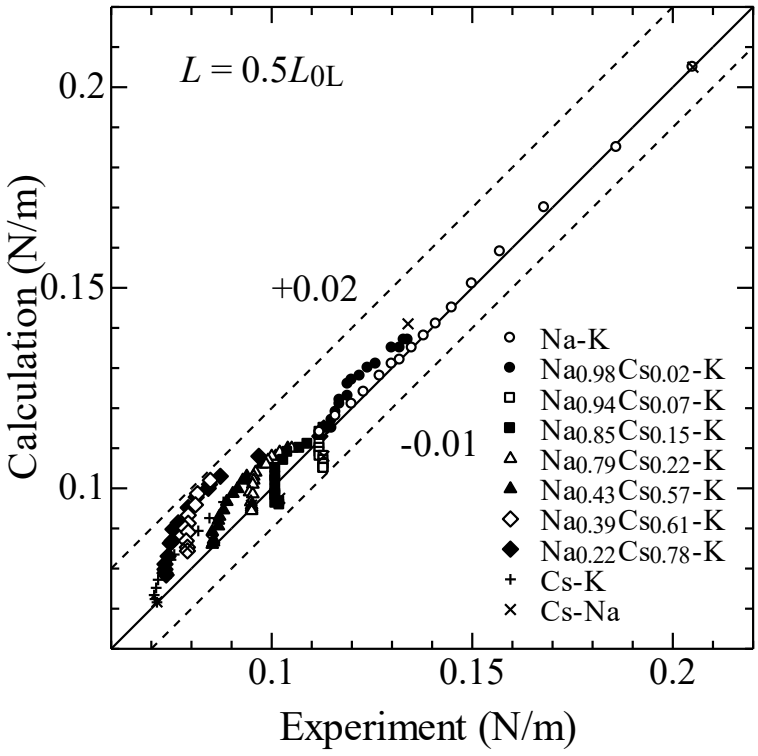

(c) $L = 0.5L_0$

Figure 9. Surface tension compared between the experiment and calculation in Na-K-Cs liquids at $T = 373$ K, which were calculated under conditions of the same Cs-Na ratio of surface concentration as the bulk ratio.

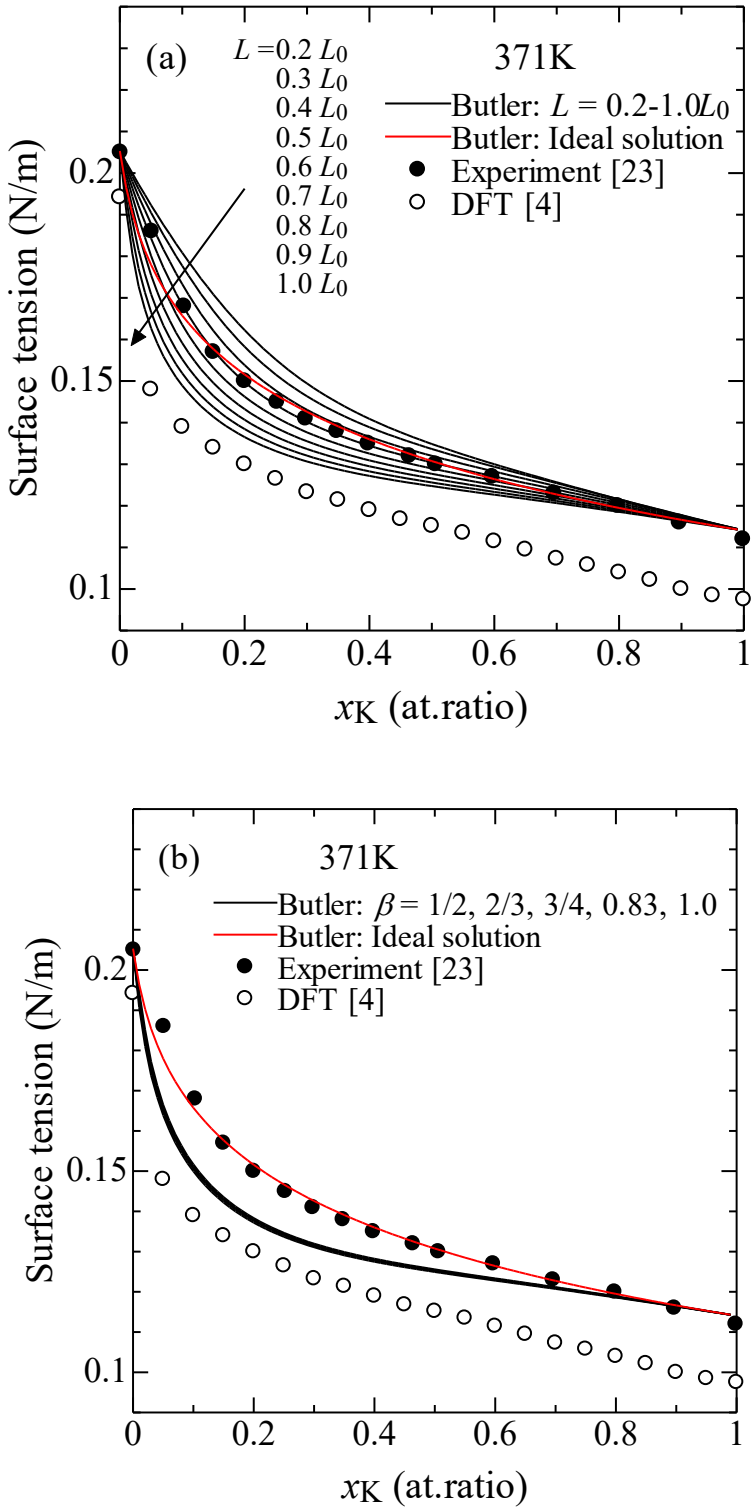

Figure 10. K-concentration dependence of Na-K surface tension at 371 K obtained by the Butler model calculation with (a) $L = 0.2L_0$ – $1.0L_0$ ($L_0 = 1.0$) and (b) $\beta = 1/2, 2/3, 3/4, 0.83, 1.0$, and the DFT calculation [4] at 371 K. The experimental temperature is 373 K [23].

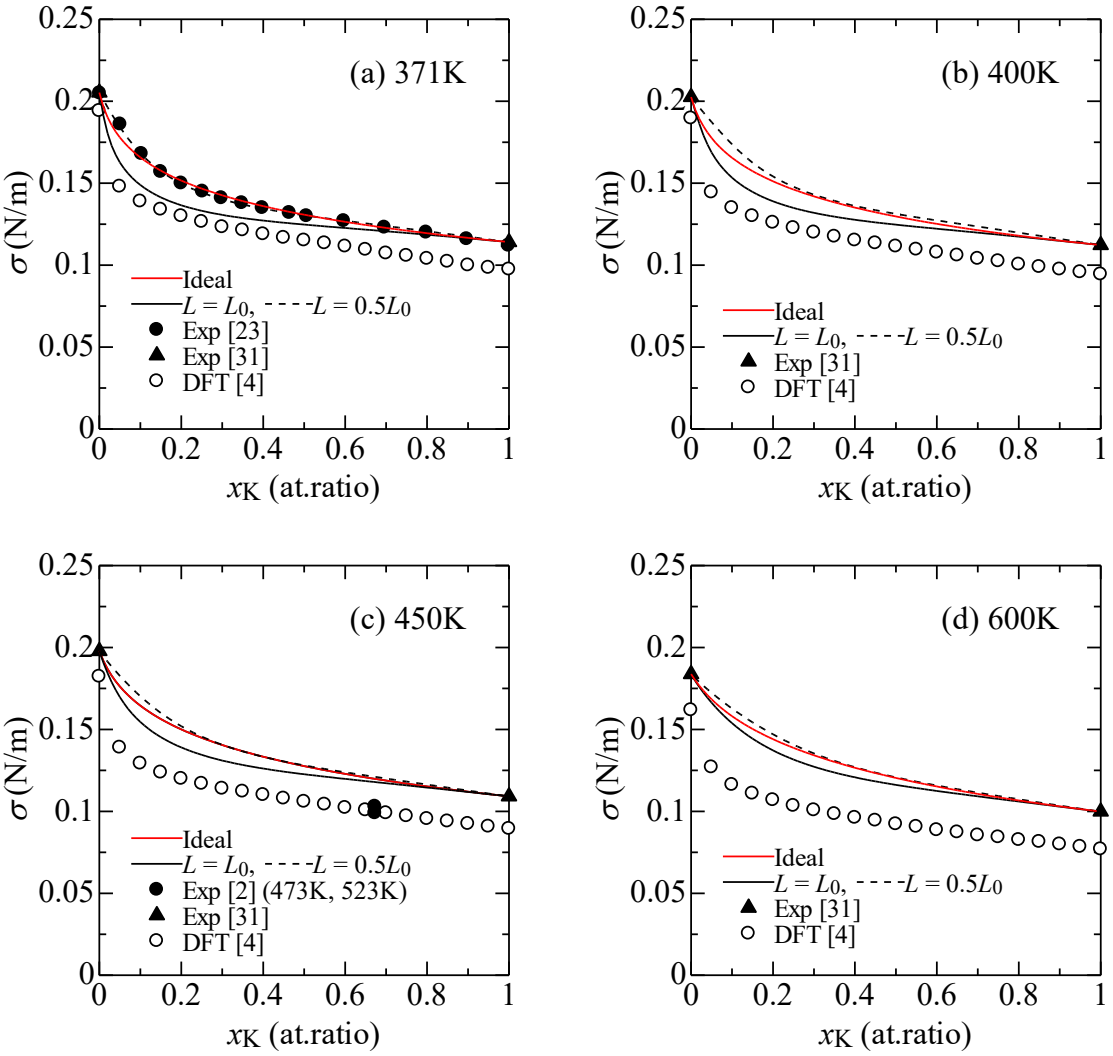

Figure 11. Temperature dependence of Na-K surface tension obtained by the Butler model calculation with $L = L_0$ and $0.5L_0$, and the DFT calculation [4] at (a) 371 K, (b) 400 K, (c) 450 K, and (d) 600 K.